Protein Engineering, Design & Selection, 2017, vol. 30 no. 11, pp. 743–751
doi: 10.1093/protein/gzx055
Advance Access Publication Date: 7 November 2017
Original Article

Original Article

Rational design of *Pleurotus eryngii* versatile ligninolytic peroxidase for enhanced pH and thermal stability through structure-based protein engineering

Yu Gao[1], Jian-Jun Li[2,*], Lanyan Zheng[1,*], and Yuguang Du[2]

[1]Department of Microbiology and Parasitology, China Medical University, No. 77 Puhe Road, Shenyang 110122, Liaoning Province, China, and [2]National Key Laboratory of Biochemical Engineering, National Engineering Research Center for Biotechnology (Beijing), Key Laboratory of Biopharmaceutical Production & Formulation Engineering, PLA, Institute of Process Engineering, Chinese Academy of Sciences, No. 1 North 2nd Street, Beijing 100190, China

[*]To whom correspondence should be addressed. E-mail: jjli@ipe.ac.cn (Jian-Jun Li); lyzheng@cmu.edu.cn (Lanyan Zheng).

Paper Edited By: Kam-Bo Wong, Board Member for PEDS

Received 3 July 2017; Revised 8 September 2017; Editorial Decision 29 September 2017; Accepted 4 October 2017

Abstract

Versatile peroxidase (VP) from Pleurotus eryngii is a high redox potential peroxidase. It has aroused great biotechnological interest due to its ability to oxidize a wide range of substrates, but its application is still limited due to low pH and thermal stability. Since CiP (Coprinopsis cinerea peroxidase) and PNP (peanut peroxidase) exhibited higher pH and thermal stability than VP, several motifs, which might contribute to their pH and thermal stability, were identified through structure and sequence alignment. Six VP variants incorporating the beneficial motifs were designed and constructed. Most variants were nearly completely inactivated except V1 (Variant 1) and V4. V1 showed comparable activity to WT VP against ABTS, while V4 exhibited reduced activity. V1 displayed improved pH stability than WT VP, at pH 3.0 in particular, whereas the pH stability of V4 did not change a lot. The thermal stabilities of V1 and V4 were enhanced with T_{50} raised by 3°C. The results demonstrated that variants containing the beneficial motifs of CiP and PNP conferred VP with improved pH and thermal stability.

Key words: Ca^{2+} binding site, pH and thermal stability, protein engineering, structure and sequence alignment, versatile peroxidase

Introduction

Lignin removal is a key procedure in the full use of cellulose and hemicellulose to produce high value-added products (Capolupo and Faraco, 2016; Bilal *et al.*, 2017; Gall *et al.*, 2017). In recent years, people have showed increased interest in lignin biodegradation for its high efficiency and low environmental pollution (Ruiz-Dueñas and Martínez, 2009; Capolupo and Faraco, 2016; Bilal *et al.*, 2017; Gall *et al.*, 2017). Some ligninolytic enzymes have been discovered and identified, which can degrade high redox potential lignin effectively, including lignin peroxidase (LiP), manganese peroxidase (MnP) and versatile peroxidase (VP) (Ruiz-Dueñas and Martínez, 2009). Among them, VP is receiving great concern due to its ability to directly oxidize a variety of substrates, including lignin, phenolic and non-phenolic aromatic compounds, and various dyes (Ruiz-Dueñas and Martínez, 2009). VP were found in *Pleurotus*, *Bjerkandera* and some other basidiomycetes (Martinez *et al.*, 1996; Mester and Field, 1998). As a Class II heme peroxidase (Hofrichter *et al.*, 2010), VP combines catalytic properties of MnP and LiP,

containing a heme cofactor located inside an internal cavity, two structural Ca^{2+} binding regions at the distal and proximal sides of the heme cavity, and different oxidation sites for different substrates like Mn^{2+}, high and low redox potential substrates, etc. (Pérez-Boada *et al.*, 2005; Ruiz-Dueñas *et al.*, 2009). There have been many studies towards VP, including heterologous overexpression (Garcia-Ruiz *et al.*, 2010; Bao *et al.*, 2012), enzymology (Martinez *et al.*, 1996; Bao *et al.*, 2012), crystallization (Pérez-Boada *et al.*, 2005), investigation into the structure–function relationship (Ruiz-Duenas *et al.*, 2007, 2008; Gao *et al.*, 2016) and protein engineering (Garcia-Ruiz *et al.*, 2010, 2012; Bao *et al.*, 2014; Gonzalez-Perez *et al.*, 2014, 2016; Sáez-Jiménez *et al.*, 2015a, 2015b, 2016).

However, VP is unstable under various conditions such as high hydrogen peroxide concentration, high temperature, and alkaline or neutral pH environment. Therefore, VP still has not been widely used in industry (Valderrama *et al.*, 2002; Verdin *et al.*, 2006; Martínez *et al.*, 2009; Garcia-Ruiz *et al.*, 2010, 2012; Bao *et al.*, 2014; Gonzalez-Perez *et al.*, 2014, 2016; Sáez-Jiménez *et al.*, 2015a, 2015b, 2016).

Some heme peroxidases like CiP (*Coprinopsis cinerea* peroxidase) and peanut peroxidase (PNP) exhibited higher thermal and alkaline stability than VP. (i) CiP belongs to class II heme peroxidases too, and has found some applications in several aspects, for instance, removal of phenolic compounds from aqueous solutions and waste waters, and as a detergent additive, etc. (Ikehata *et al.*, 2005). CiP has a 40 ± 45% identity in amino acid sequence and a similar tertiary structure to LiP (Petersen *et al.*, 1994). Importantly, this enzyme is very stable at high pH values, for example, peroxidases from *Coprinus* (*Coprinopsis*) sp. UAMH 10 067 and *Coprinus cinereus* (*Coprinopsis cinerea*) UAMH 4103 retained about 95% and 60% of original activity, respectively, even at pH 10 after several days (Ikehata *et al.*, 2005). The inactivation temperature of CiP was reported to be around 65°C (McEldoon and Dordick, 1996). What's more, its oxidative, alkaline and thermal stability was further improved by directed evolution (Cherry *et al.*, 1999). (ii) Both PNP and horseradish peroxidase (HRP) belong to Class III heme peroxidase (Hofrichter *et al.*, 2010). Notably, when two calcium ions were completely removed from HRP and PNP, both were still 40% and 50% active, respectively (Shiro *et al.*, 1986; Hu *et al.*, 1987; Schuller *et al.*, 1996). At 60°C, PNP lost about 65–70% of original activity (Lige *et al.*, 2001).

In contrast, the high redox potential peroxidases like VP, LiP and MnP were completely inactivated when they were incubated at pH 8.0 for some time (Sutherland and Aust, 1996; George *et al.*, 1999; Reading and Aust, 2000; Gao *et al.*, 2016). The threshold for inactivation of MnP and VP was found to be temperatures higher than 40°C (Reading and Aust, 2000; Garcia-Ruiz *et al.*, 2012). Previous results have demonstrated that thermal and pH stabilities of ligninolytic peroxidases are closely related to two structural Ca^{2+} (George *et al.*, 1999; Garcia-Ruiz *et al.*, 2010; Gao *et al.*, 2016).

In this study, based on the structure and sequence alignment of CiP and VP, PNP and VP, some variants incorporating the beneficial motifs of PNP and CiP into VP, which might contribute to their pH and thermal stability, were designed, made and fully characterized.

Materials and Methods

Materials

Chemicals were from Sigma (St. Louis, Missouri, USA) and Merck (New Jersey, USA). Oligonucleotides were synthesized by Shanghai Sangon Biotech Co. Ltd (China). *Pfu* DNA polymerases from Fermentas (Pittsburgh, Pennsylvania, USA). *Dpn*I was from New England BioLabs (Ipswich, Massachusetts, USA). Plasmid Mini Kit I was from Omega Bio-tek (Norcross, Georgia, USA), and Competent Cell Preparation Kit was from Takara Biotechnology (Otsu, Shiga, Japan). Nickel column was from Novagen (Frankfurter Straße, Darmstadt, Germany). Super GelRed was purchased from US Everbright (China).

Bacterial strains, plasmids and media

E. coli DH5α was used for routine DNA transformation and plasmid isolation. *E. coli* BL21(DE3) was utilized for VP overexpression. *E. coli* strains were routinely grown in Luria-Bertani broth at 37°C with aeration or on LB plates supplemented with 1.5% (w/v) agar. About 100 μg/ml Ampicillin was added when required.

DNA manipulations

General molecular biology techniques were carried out by following standard procedures (Sambrook *et al.*, 1989). Plasmid DNA was isolated using the Plasmid Mini Kit I.

Alignment of VP, CiP and PNP, and construction of variants

Primary amino acid sequences of VP, CiP and PNP were aligned using Clustal Omega (http://www.ebi.ac.uk/Tools/msa/clustalo/), and structural alignment of VP (PDB code: 2BOQ), CIP (PDB code: 1H3J) and PNP (PDB code: 1SCH) were performed with PyMOL. V1 and V2 were constructed through prolonged overlap extension PCR (Ho *et al.*, 1989). Since a lot of mutations were involved in V2, the modified region was divided into two parts. After one part was modified successfully, this part was used as the template for the second part. V3, V4, V5 and V6 were made according to the standard QuickChange Site-Directed Mutagenesis protocol (Stratagene Ltd., La Jolla, California, USA), among which V4 was constructed by two rounds of PCRs. All primers were listed in Table S1 in Supplementary Materials. The required modifications were confirmed by DNA sequencing.

Protein overexpression and purification

WT VP and all variants were overexpressed in *E. coli* BL21(DE3) in the presence of heme under IPTG induction following published procedure (Bao *et al.*, 2012, 2014; Gao *et al.*, 2016). WT VP and all variants were purified on Nickel column as reported (Bao *et al.*, 2012, 2014; Gao *et al.*, 2016). The purity of protein was checked by SDS-PAGE. The protein concentration was determined by the Bradford method using bovine serum albumin as a standard. Each enzyme was estimated to be >90% pure by SDS-PAGE. The R_z value was calculated based on $A_{407\,nm}/A_{280\,nm}$.

Enzyme activity assay

H_2O_2 concentration was estimated by titration using potassium permanganate, and further checked spectrophotometrically based on $\varepsilon_{240\,nm} = 43.6\ M^{-1}\ cm^{-1}$ (Hiner *et al.*, 2000).

The enzymatic assays against ABTS (2,2′-azinobis (3-ethylbenzothiazoline-6-sulfonate)), Mn^{2+}, veratryl alcohol and Reactive Black 5 were carried out according to the published procedures (Bao *et al.*, 2012, 2014; Gao *et al.*, 2016). One unit of enzyme activity (U) is defined as the amount of the enzyme that catalyzes conversion

of 1 μmol substrate per min. The K_m and V_{max} values for ABTS were determined by fitting the Michaelis–Menten equation using GraphPad Prism (GraphPad Co. Ltd., USA). The k_{cat} values were calculated from V_{max} on the basis of 52.6 kDa, which was predicted based on the amino acid sequence of VP fused to thioredoxin. All enzymatic assays were done in triplicate.

UV–vis spectroscopy

UV–visible spectra for all variants and WT VP were recorded between 250 nm and 700 nm on a multimode reader (Infinite M200 PRO, TECAN) in 10 mM sodium tartrate (pH 5.5) at 25°C. The protein concentrations were as follows (in mg/ml): V1, 0.78; V2, 0.74; V3, 0.85; V4, 0.79; V5, 0.61; V6, 0.91; WT VP, 0.85.

Determination of optimal pH and pH stability

The pH-rate profiles of WT VP and variants were determined using 0.5 mM ABTS as the substrate in 0.1 M B & R (Britton and Robinson) buffer containing 0.1 mM H_2O_2 over the pH ranges of pH 2.0 to 9.0 at 418 nm and 25°C (Britton and Robinson, 1931).

The pH stability was estimated by first preincubating the purified enzymes in 0.1 M B & R buffer at different pH values (pH 2.0 to 9.0). Then the residual activities were measured against 0.5 mM ABTS in 0.1 M sodium tartrate (pH 3.5) containing 0.1 mM H_2O_2 at 25°C immediately after incubated at 4°C for 1 min, 1 h, 4 h, 25 h and 120 h, respectively. For each enzyme, the highest activity was taken as 100%, and the percentage of the residual activity at different time points and pH values against the highest one was calculated. All enzymatic assays were performed in triplicate.

Determination of thermal stability

The thermostabilities of WT and variants were estimated by measuring the T_{50} value using 96-well gradient thermocyclers (TC-5000, TECHNE), which was defined as the temperature at which enzyme loses 50% of original activity following incubated for 10 min. After

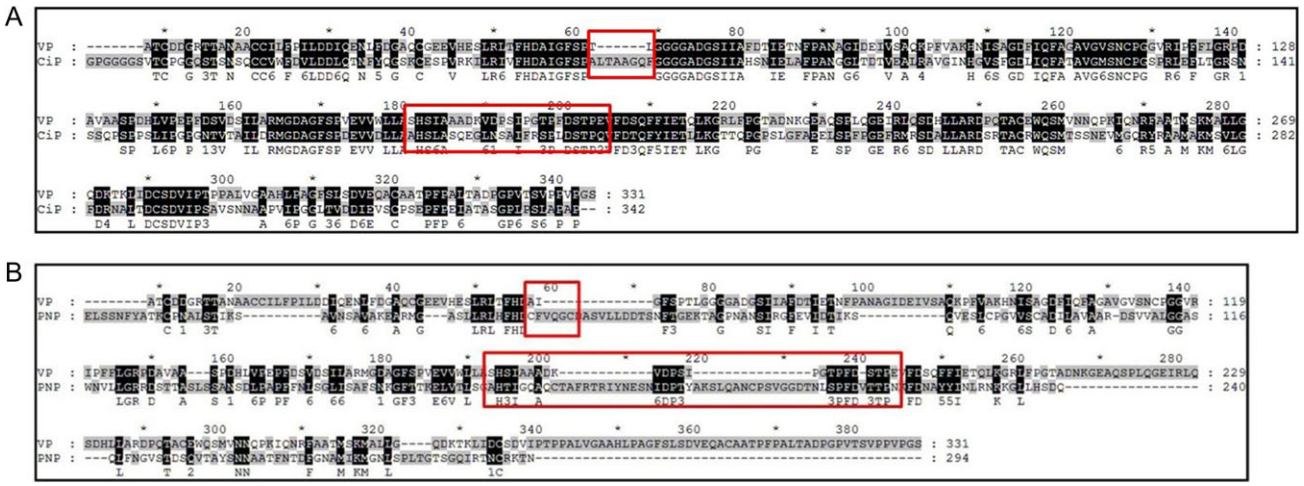

Fig. 1 Sequence alignment of VP and CiP (**A**), VP and PNP (**B**). The differences in the loop around two structural Ca^{2+} binding sites were highlighted with red rectangles

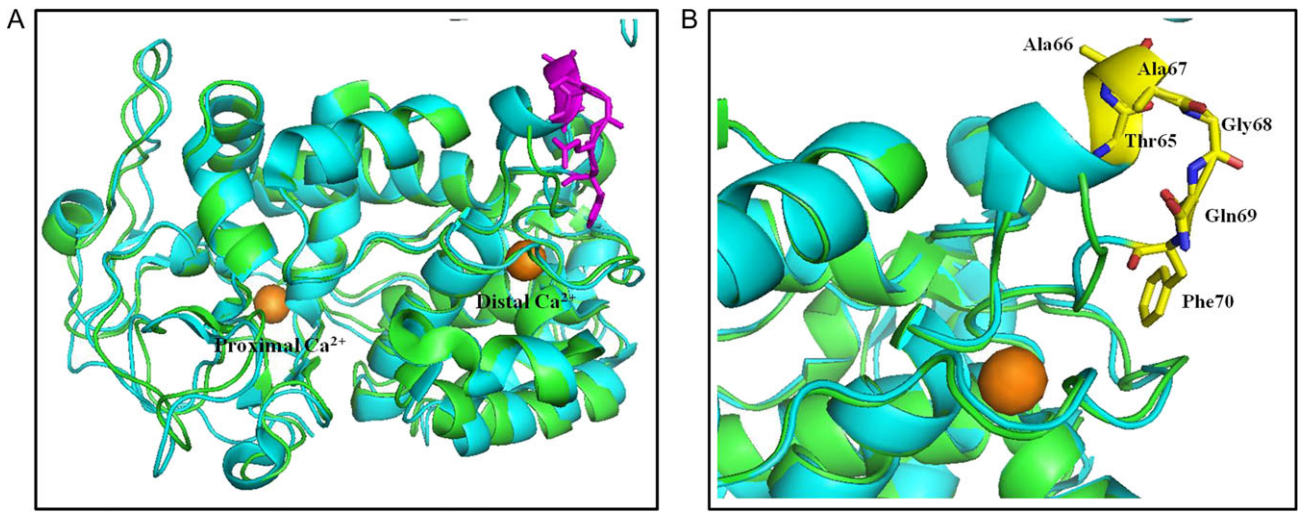

Fig. 2 Structure superimposition of VP (PDB code: 2BOQ) and CiP (PDB code: 1H3J): full (**A**) and the part around the distal Ca^{2+} binding site (**B**). The different motif was highlighted with magenta. Crystal structures of VP and CiP were shown in green and cyan, respectively

some trials, the enzymes were incubated for 10 min in a gradient temperature ranging from 40°C to 70°C for WT VP and variants. After 10 min of incubation, enzymes were chilled on ice for 10 min and further incubated for 5 min at room temperature. Afterwards aliquots (50 µl) were subjected to the ABTS-based assay described above. The thermostability values were deduced from the ratio between the residual activities incubated at different temperature points and the initial activity. All enzymatic assays were carried out in triplicate.

Circular dichroism spectroscopy

Far-UV circular dichroism (CD) spectra (190 to 260 nm) were recorded for WT VP and variants at 0.05 mg/ml in 50 mM citrate-phosphate buffer (pH 5.5) on a Jasco J-810 spectropolarimeter at 25°C. Data were averaged over three runs and the background was subtracted.

Secondary-structure analyses were performed with the BeStSel method, which is available at the bestsel.elte.hu server (Micsonai *et al.*, 2015).

Results

Identification of the target residues for mutagenesis

Since it was observed that CiP and PNP exhibited higher alkaline and thermal stability than VP (Shiro *et al.*, 1986; Hu *et al.*, 1987; Schuller *et al.*, 1996), they might contain some structural motifs beneficial to their stability. The sequence and structure alignment of VP (PDB code: 2BOQ) and CiP (PDB code: 1H3J) showed that the amino acid sequences around the proximal calcium region were not highly conservative (The sequence identity between VP and CiP is 49.2%.) (Figs 1A and 2), and the loop structures around the distal calcium region were quite different: CiP has six amino acids (Thr65, Ala66, Ala67, Gly68, Gln69 and Phe70) longer loop than VP (Figs 1A and 2). In contrast, the sequence identity between VP and PNP is only 27.3% (Fig. 1B), and superimposition of the crystal structures of VP and PNP (PDB code: 1SCH) revealed that PNP has seven amino acids (Ser53, Pro54, Thr55, Leu56, Gly57, Gly58 and Gly69) shorter loop than VP, separating the residues which make up the distal calcium site (Fig. 3). In addition, in PNP there was a disulfide bond between Cys44 and Cys49 close to two ligands of the distal

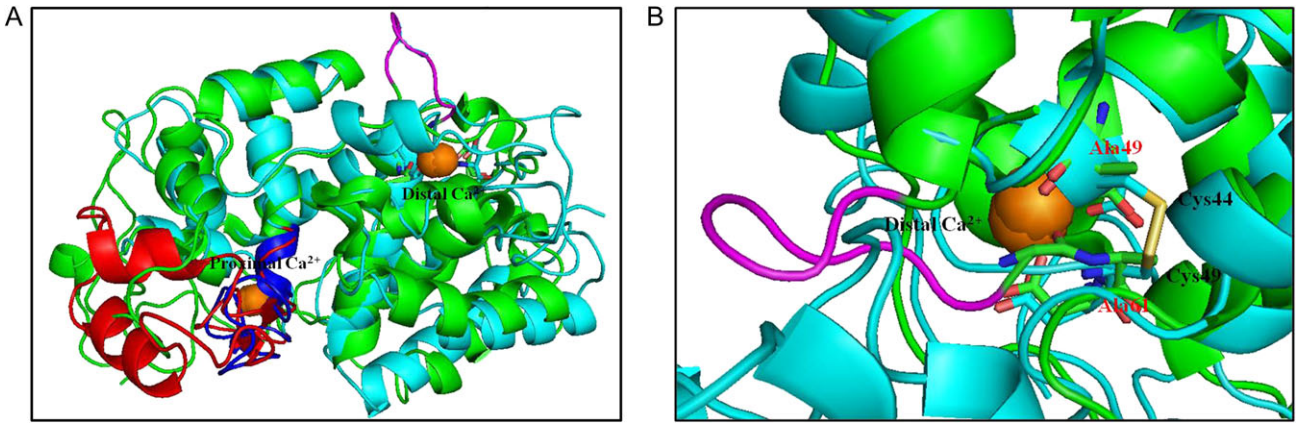

Fig. 3 Structure superimposition of VP (PDB code: 2BOQ) and PNP (PDB code: 1SCH): full (**A**) and the part around the distal Ca^{2+} binding site (**B**).The different motifs were highlighted with magenta, red and blue, respectively. Crystal structures of VP and PNP were shown in green and cyan, respectively

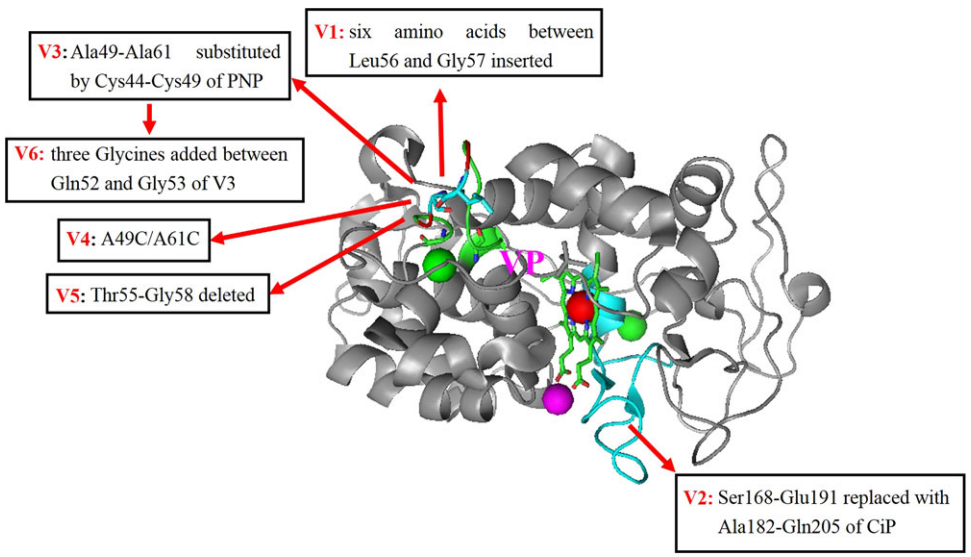

Fig. 4 A scheme representing the different structural motifs introduced into VP variants

calcium ion—Asp43 and Asp50, forming a loop encompassing several of the distal calcium ligand residues (Schuller *et al.*, 1996). However, none of the class I or II peroxidases contains the equivalent of the disulfide Cys44-Cys49 in PNP (Schuller *et al.*, 1996). A similar disulfide bond and a much shorter loop around the distal calcium site are also present in HRP (Gajhede *et al.*, 1997). This might be the reason why rigorous conditions were required to release Ca^{2+} from PNP and HRP (Shiro *et al.*, 1986; Hu *et al.*, 1987; Schuller *et al.*, 1996). Based on this observation, the thermal and pH stability of MnP was improved by engineering such a disulfide bond around distal calcium site in MnP (Reading and Aust, 2000). Moreover, there is a big difference in the loop around proximal Ca^{2+} between VP and PNP according to the sequence and structure alignment (Figs 1B and 3).

All these above different motifs among these enzymes, which might be related to higher pH and thermal stability of CiP and PNP (Shiro *et al.*, 1986; Hu *et al.*, 1987; Schuller *et al.*, 1996), were integrated into VP to see whether these beneficial motifs could confer VP with improved stability in this study.

Construction, overexpression and purification of variants

Based on the different motifs between VP and CiP, VP and PNP, six variants were designed and constructed (Fig. 4). For V1 (Variant 1), six amino acids of CiP (Thr65, Ala66, Ala67, Gly68, Gln69 and Phe70) were inserted between Leu56 and Gly57 around distal Ca^{2+} in VP to imitate the longer loop in CiP. In V2, the residues Ser168-Glu191 of VP around proximal Ca^{2+} were replaced with Ala182-Gln205 of CiP to simulate the loop of CiP. In the case of V3, Ala49-Ala61 of VP were substituted by Cys44-Cys49 of PNP to mimic the shorter loop around distal Ca^{2+} in PNP. As far as V4 is concerned, both Ala49 and Ala61 in VP were mutated into Cysteine to generate a disulfide bond between them, similar to the one existing between Cys44 and Cys49 in PNP (Schuller *et al.*, 1996). For V5, Thr55-Gly58 of VP were removed to obtain a truncated loop for a tighter structure around the distal calcium region to mimic the shorter loop of PNP. For CP V6, three Glycines were inserted between Gln52 and Gly53 in V3 to generate a more flexible loop. All variants were successfully overexpressed in *E. coli* BL21(DE3), and purified on nickel column as before (Fig. S1).

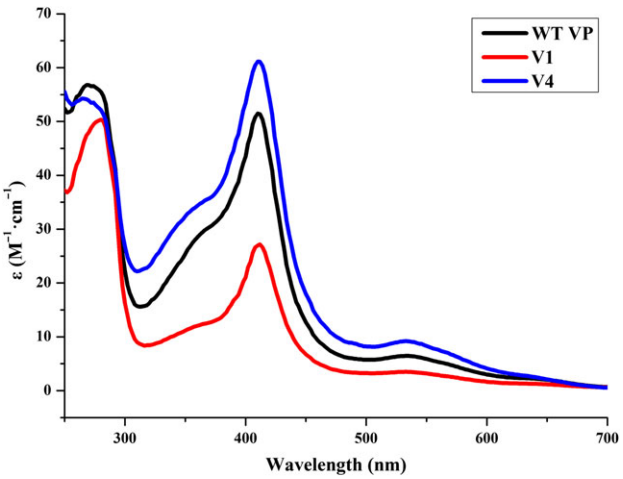

Fig. 5 UV–Vis spectra of wild-type VP, V1 and V4. UV–visible spectra were scanned between 250 nm and 700 nm in 10 mM sodium tartrate (pH 5.5). The protein concentrations (mg/ml) were as follows: WT VP, 0.85; V1, 0.78; V4, 0.79

Spectroscopic studies

UV–visible spectra for all variants and WT VP were recorded between 250 nm and 700 nm on a multimode reader (Fig. 5, Fig. S2). No obvious peak was observed around 500 nm (corresponding to CT2 band, charge transfer band) for WT, and three peaks appeared at 536 nm, 564 nm and 636 nm, which were ascribed to β, α and CT1 bands, respectively (Fig. S2) (Pérez-Boada *et al.*, 2005; Saez-Jimenez *et al.*, 2015a; Gao *et al.*, 2016). All variants displayed similar absorption spectra to WT VP (Fig. 5, Fig. S2). Only a slight red shift (around 2 nm) was observed in the Soret band in all variants except V4. A clear increase at 532 nm was found in V3 and V6, while a slight decrease in V1 was observed (Fig. 5, Fig. S2).

Enzymatic activities of WT VP and variants

The specific activities of WT VP and variants against four different substrates were shown in Table I. Substrates are oxidized at different sites in VP: (i) High redox potential VA (veratryl alcohol) and RB5 (Reactive Black 5) are oxidized at the catalytic tryptophan; (ii) Though low redox potential ABTS could be oxidized both at the catalytic tryptophan (the high efficiency site) and at the heme channel (the low efficiency site), only the activity at the low efficiency site was assayed for ABTS in the current study; (iii) Mn^{2+} is oxidized at the Mn^{2+}-binding site (Ruiz-Dueñas *et al.*, 2009).

Most variants showed greatly reduced activities except V1 and V4. Compared with WT VP, V2 and V5 lost >97% of original activity against $MnSO_4$. When ABTS was used as the substrate, the activity of V1 was not affected greatly, retaining about 108% and 85% of WT VP activity, respectively, and V4 only retained about

Table I. Specific activities determined against different substrates[a].

Variants	R_z	Specific activity (U/mg (% of WT))			
		ABTS	RB5	VA	Mn^{2+}
WT	0.90	0.60 ± 0.08 (100)	0.044 ± 0.005 (100)	0.053 ± 0.006 (100)	3.00 ± 0.4 (100)
V1	1.05	0.65 ± 0.07 (108)	0.018 ± 0.003 (41)	0.029 ± 0.004 (55)	1.60 ± 0.3 (53)
V2	1.15	NA	NA	NA	0.04 ± 0.008 (1.3)
V3	1.21	NA	NA	NA	NA
V4	1.09	0.17 ± 0.02 (28)	0.033 ± 0.005 (75)	0.031 ± 0.005(58)	2.63 ± 0.4 (88)
V5	1.34	NA	NA	NA	0.07±0.01(2.3)
V6	1.08	NA	NA	NA	NA

[a]All enzymatic assays were done in triplicate.

28%. However, the activities of V1 and V4 against other substrates were reduced to different extent. For V1, the bigger influence on oxidation of VA, RB5 and MnSO4 was observed than on oxidation of ABTS; For V4, the impact on oxidation of ABTS was greater than on oxidation of VA, RB5 and $MnSO_4$.

Since most variants' specific activities were so low that their steady-state kinetics could not be measured, only the kinetic parameters of VP, V1 and V4 were determined (Table II). Compared with WT VP, the kinetic parameters, including K_m, k_{cat} and catalytic efficiency (k_{cat}/K_m), were not affected too much for V1, whereas the K_m value of V4 was increased slightly and its k_{cat} and catalytic efficiency (k_{cat}/K_m) were reduced significantly.

Table II. Kinetic parameters of WT VP, V1 and V4[a]

	K_m (μM)	k_{cat} (s^{-1})	k_{cat}/K_m (s^{-1} μM^{-1})
WT	1.26 ± 0.10	0.53 ± 0.02	0.42
V1	1.53 ± 0.13	0.57 ± 0.02	0.37
V4	1.61 ± 0.12	0.04 ± 0.00	0.02

[a]ABTS was used as the substrate, and all enzymatic assays were carried out in triplicate.

pH optima and stabilities of WT VP and variants

The pH-activity profiles for WT VP, V1 and V4 were made over the pH ranges 2.0–9.0 (Fig. S2). The optimal pH values of V1, and V4 were at pH 3.0, similar to that of WT VP. Both variants displayed higher activities over a narrow pH range than WT VP. As shown in Fig. S3, when pH is above 6.0 or at 2.0, all enzymes nearly completely lost their activities.

The pH stabilities of WT VP, V1 and V4 over the pH ranges of 2.0–9.0 were determined (Fig. 6). At pH 2.0, 8.0 and 9.0, both variants were almost completely inactive after 1 h incubation. Just as reported, WT VP was relatively stable in the pH ranges of 3.5–7.0, retaining 60–80% of initial activity after 120 h incubation (Gao *et al.*, 2016). At pH 3.5 to pH 7.0, the stabilities of V1 and V4 were comparable to that of WT VP, retaining 60–80% of original activity after 120 h incubation. In the case of stability at pH 3.0, there were some differences among V1, V4 and WT VP. The residual activities at pH 3.0 were increased from 40% in WT VP to 60% in V1 and

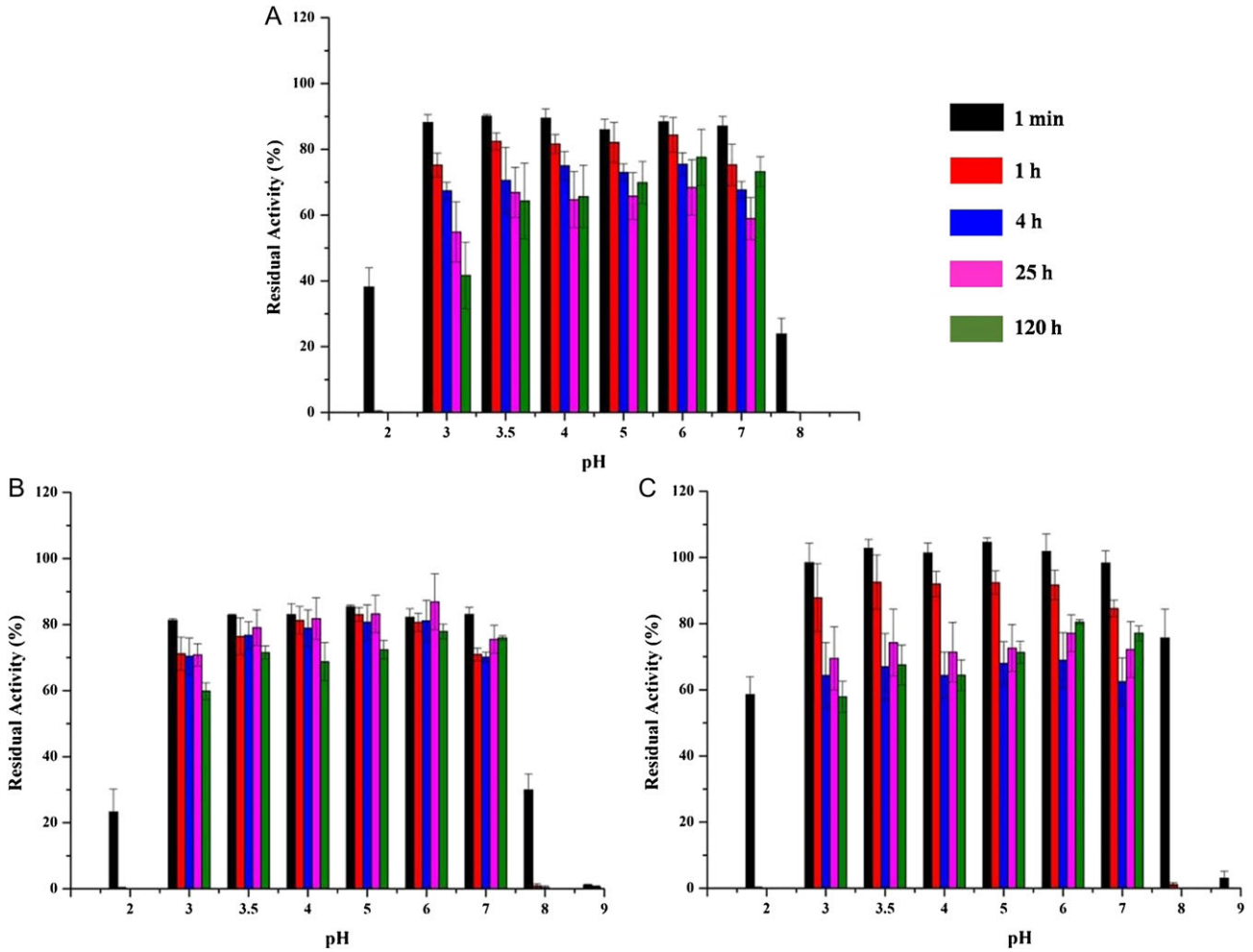

Fig. 6 pH stabilities of WT VP and three variants: (**A**) WT, (**B**) V1, (**C**) V4. The pH stability was estimated by first preincubating the purified enzymes in B&R (Britton and Robinson) buffer at different pH values (pH 2.0 to 9.0). Then the residual activities were estimated using 0.5 mM ABTS in 0.1 M sodium tartrate (pH 3.5) containing 0.1 mM H_2O_2 at 25°C immediately after incubation at 4°C for 1 min, 1 h, 4 h, 25 h and 120 h, respectively. All enzymatic assays were performed in triplicate

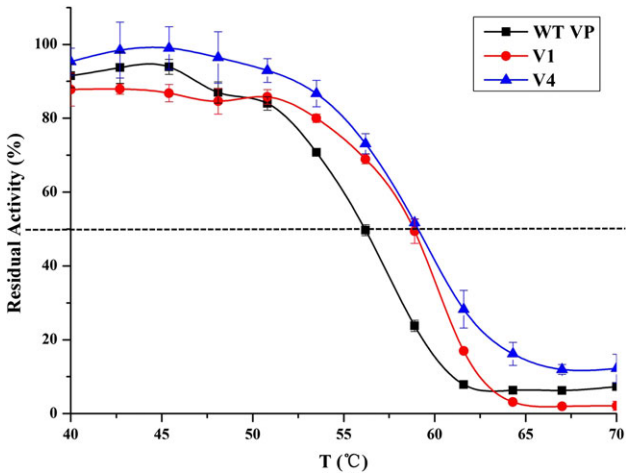

Fig. 7 Thermostabilities of wild-type VP and some variants. Each point, including the standard deviation, was from three independent experiments. The enzymes were incubated for 10 min in a gradient temperature ranging from 40°C to 70°C for WT VP, V1 and V4. After 10 min of incubation, samples were chilled on ice for 10 min and further incubated for 5 min at rt. Afterwards aliquots (50 µl) were subjected to the ABTS-based assay. All enzymatic assays were done in triplicate

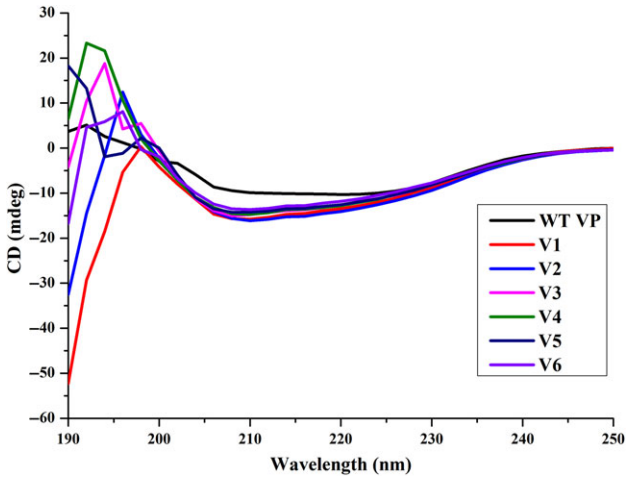

Fig. 8 CD spectra of WT VP and variants. Far-UV CD spectra (190–260 nm) were recorded for protein samples (0.05 mg/ml) in 15 mM citrate-phosphate buffer (pH 5.5) at 25°C

Table III. Secondary-structure (%) estimation based on CD spectra of WT VP and variants. Secondary-structure analyses were performed with BeStSel method (Micsonai *et al.*, 2015)

	α Helix	β Strand		Turn	Others
		Antiparallel	Parallel		
WT	11.4	21.6	12	13.5	41.5
V1	15.6	15.1	11.1	13.6	44.5
V2	11.8	17.3	12.3	12.4	46.2
V3	9.7	17.6	10.4	14,6	47.8
V4	12.9	14.9	9.5	15.2	47.5
V5	10.4	17.1	11.2	13.9	47.3
V6	10.2	20.1	9.9	12.9	47.0

V4, suggesting a slight improvement in acidic stability for these two variants.

Thermal stability assay

T_{50}, defined as the temperature at which the enzyme loses 50% of original activity following incubated for 10 min, was used to estimate the thermostabilities of WT, V1 and V4 (Fig. 7). In comparison with WT VP, the T_{50} values of both V1 and V4 were increased from 56°C to 59°C. Though the T_{50} values of V1 and V4 were not raised significantly, the activity at specific temperature was greatly enhanced. For example, the activities of V1 and V4 were about 2.5-fold higher that of WT VP at 58°C (Fig. 7).

CD for WT VP and variants

CD was used to investigate the effects of mutations on the conformational or secondary structure. All variants and WT VP showed similar CD spectra and secondary structures (Fig. 8, Table III).

Discussion

VP, as a type of newly discovered high redox potential ligninolytic peroxidase, received great attention due to its catalytic promiscuity (Ruiz-Dueñas and Martínez, 2009). However, its instability under some conditions such as high hydrogen peroxide concentration, high temperature, and strong acids or bases limits its industrial applications (Valderrama *et al.*, 2002; Verdin *et al.*, 2006; Garcia-Ruiz *et al.*, 2010, 2012; Bao *et al.*, 2014; Gonzalez-Perez *et al.*, 2014, 2016; Sáez-Jiménez *et al.*, 2015a, 2015b, 2016). Therefore, there is an urgent need to enhance its stability (Garcia-Ruiz *et al.*, 2010, 2012; Bao *et al.*, 2014; Gonzalez-Perez *et al.*, 2014, 2016; Sáez-Jiménez *et al.*, 2015a, 2015b, 2016).

Considering the fact that CiP and PNP exhibited higher thermal and alkaline stability than VP (Shiro *et al.*, 1986; Hu *et al.*, 1987; McEldoon and Dordick, 1996; Schuller *et al.*, 1996; Lige *et al.*, 2001; Ikehata *et al.*, 2005), and VP showed high structure identity to CiP and PNP and high sequence identity to CiP (Petersen *et al.*, 1994; Schuller *et al.*, 1996), structure- and sequence-based engineering strategy was utilized to improve VP's pH and thermal stability in the current study. Six VP variants V1, V2, V3, V4, V5 and V6, incorporating the beneficial structural motifs contributing to the pH and thermal stability of CiP and PNP into VP, were designed, constructed and fully characterized.

Variants performed differently against four types of substrates tested, which were oxidized at different catalytic sites (Ruiz-Dueñas *et al.*, 2009). The studies towards V3, V5 and V6 demonstrated that truncation of the loop around distal Ca^{2+} in VP impaired activities significantly. Since it has been suggested that the redox potential and activation of peroxidases by H_2O_2 depend on the precise position of two histidines located immediately below and above the heme cofactor, the complete loss of activities of V3, V5 and V6 may be because the distal calcium region and/or the position of the distal histidine (His47) in helix B was/were destabilized by the truncated loop around distal Ca^{2+} (Sáez-Jiménez *et al.*, 2015b). The results of V2 indicated that substitution of Ser168-Glu191 around proximal Ca^{2+} in VP by Ala182-Gln205 in CiP had big effects on catalytic activities, suggesting that the side chains of those nonconserved amino acids around proximal Ca^{2+} in VP may play important roles in maintaining VP activity. In addition, it has been observed that the stabilization of the environment of the proximal histidine (His169 acting as the fifth heme iron ligand, located at helix F) is critical

taking into consideration that the strength of the interaction between His169 and the heme iron has been proposed as one of the factors determining the high redox potential of ligninolytic peroxidases (Banci *et al.*, 1991, 2003). Thus, nearly completely inactivated V2 could possibly result from destabilization of the environment of this proximal histidine.

The results of V1 implied that introduction of additional six amino acids between Leu56 and Gly57 around distal Ca^{2+} in VP led to reduced activities towards Mn^{2+} and high redox potential RB5 and VA, and did not influence oxidation of low redox potential ABTS at the high efficiency site. As expected, V1, which incorporated the potential beneficial motif of CiP to stability into VP, exhibited higher acidic stability (pH 3.0) and thermal stability than WT VP. The results demonstrated that extension of six amino acids for the loop around distal Ca^{2+} in VP improved acidic and thermal stability of VP. In the case of V4, generation of a disulfide bond between the residues 49 and 61 around distal Ca^{2+} in VP affected oxidation of ABTS at the high efficiency site significantly, and did not affect catalytic activities against Mn^{2+} and RB5 too much. Though V4's activities towards ABTS and VA were significantly reduced, it showed enhanced thermal stability and acidic stability (pH 3.0). As reported for MnP, the results further proved that the extra disulfide bond contributed to the thermal and pH stability (Reading and Aust, 2000). Formation of that disulfide bond in VP was confirmed by the crystal structure of VPi-ss, a VP variant containing eight mutations (D69S/T70D/S86E/D146T/Q202L/H232E/Q239R/S301K) in addition to A49C and A61C. Although the two new cysteines are situated close to the amino acids Asp48, Gly60, Asp62 and Ser64 coordinating distal Ca^{2+}, this region did not show any additional change compared with WT VP (Sáez-Jiménez *et al.*, 2015b). Our results confirmed the impact of the disulfide bond only on thermal and pH stability of VP for the first time. Given the fact that both Ca^{2+} sites are closely related with pH and thermal stability of ligninolytic peroxidases (George *et al.*, 1999; Gao *et al.*, 2016), the above results implied that insertion of six amino acids into the loop or introduction of a disulfide bond around distal Ca^{2+} in VP did not affect Ca^{2+} binding too much. The obtained effects may result from the distal calcium region and/or the position of His47 further stabilized by the newly formed disulfide bond between Cys49 and Cys61 in VP and MnP or extension of six amino acids for the loop around distal Ca^{2+} site in VP (Sáez-Jiménez *et al.*, 2015b).

V1 and V4 displayed enhanced acidic stability, especially at pH 3.0. We expected a similar effect at pH above 7.0 according to the reported results for an engineered MnP variant including a similar disulfide bond between A48C and A63C (Reading and Aust, 2000). However, both did not show increased stability at neutral and alkaline pH compared with WT VP. These differences have been proposed to result from different mechanisms responsible for pH inactivation at acidic and neutral pH (Sáez-Jiménez *et al.*, 2015b).

It seems that all variants did not show obvious changes in UV–vis spectra, CD spectra and secondary structures in comparison with WT VP, suggesting that the modifications did not lead to big structural changes.

In conclusion, according to the structure and sequence alignment among VP, CiP and PNP, six VP variants harboring the potential beneficial motifs contributing to the pH and thermal stability of CiP and PNP were designed, constructed and characterized. Most variations resulted in great loss of enzyme activities except V1 and V4. V1 and V4 displayed improved both acidic and thermal stability, and showed little effects on activity. The designed variants V1 and V4 are more stable at low pH, making them of special interest from a biotechnological point of view in processes such as ligninolysis favored by acidic conditions. The results demonstrated that the structure-based engineering strategy would be useful for rational construction of stable ligninolytic peroxidases and even other enzymes.

Supplementary Data

Supplementary data are available at *Protein Engineering, Design and Selection*.

Funding

This work was supported by National Science Foundation of China (31370799 and 31170765) and Beijing Natural Science Foundation (5162022).

References

Banci,L., Bertini,I., Turano,P., Tien,M. and Kirk,T.K. (1991) *Proc. Natl. Acad. Sci. USA.*, **88**, 6956–6960.

Banci,L., Camarero,S., Martínez,A.T., Martínez,M.J., Pérez-Boada,M., Pierattelli,R. and Ruiz-Dueñas,F.J. (2003) *J. Biol. Inorg. Chem.*, **8**, 751–760.

Bao,X., Huang,X., Lu,X. and Li,J.-J. (2014) *Enzyme Microb. Tech.*, **54**, 51–58.

Bao,X., Liu,A., Lu,X. and Li,J.-J. (2012) *Biotechnol. Lett.*, **34**, 1537–1543.

Bilal,M., Asgher,M., Iqbal,H.M., Hu,H. and Zhang,X. (2017) *Int. J. Biol. Macromol.*, **98**, 447–458.

Britton,H.T.K. and Robinson,R.A. (1931) *J. Chem. Soc.*, 1456–1462.

Capolupo,L. and Faraco,V. (2016) *Appl. Microbiol. Biotechnol.*, **100**, 9451–9467.

Cherry,J.R., Lamsa,M.H., Schneider,P., Vind,J., Svendsen,A., Jones,A. and Pedersen,A.H. (1999) *Nat. Biotechnol.*, **17**, 379–384.

Gajhede,M., Schuller,D.J., Henriksen,A., Smith,A.T. and Poulo,T.L. (1997) *Nat. Struct. Biol.*, **4**, 1032–1038.

Gall,D.L., Ralph,J., Donohue,T.J. and Noguera,D.R. (2017) *Curr. Opin. Biotechnol.*, **45**, 120–126.

Gao,Y., Zheng,L., Li,J.-J. and Du,Y. (2016) *Arch. Biochem. Biophys.*, **612**, 9–16.

Garcia-Ruiz,E., Gonzalez-Perez,D., Ruiz-Duenas,F.J., Martinez,A.T. and Alcalde,M. (2012) *Biochem. J.*, **441**, 487–498.

Garcia-Ruiz,E., Mate,D., Ballesteros,A., Martinez,A.T. and Alcalde,M. (2010) *Microb. Cell Fact.*, **9**, 17.

George,S.J., Kvaratskhelia,M., Dilworth,M.J. and Thorneley,R.N. (1999) *Biochem. J.*, **344**, 237–244.

Gonzalez-Perez,D., Garcia-Ruiz,E., Ruiz-Duenas,F.J., Martinez,A.T. and Alcalde,M. (2014) *ACS Catal.*, **4**, 3891–3901.

Gonzalez-Perez,D., Mateljak,I., Garcia-Ruiz,E., Ruiz-Dueñas,F.J., Martinez, A.T. and Alcalde,M. (2016) *Catal. Sci. Technol*, **6**, 6625–6636.

Hiner,A.N.P., Rodríguez-López,J.N., Arnao,M.B., Lloyd,R.E., García-Cánovas,F. and Acosta,M. (2000) *Biochem. J.*, **348**, 321–328.

Ho,S.N., Hunt,H.D., Horton,R.M., Pullen,J.K. and Pease,L.R. (1989) *Gene*, **77**, 51–59.

Hofrichter,M., Ullrich,R., Pecyna,M.J., Liers,C. and Lundell,T. (2010) *Appl. Microbiol. Biotechnol.*, **87**, 871–897.

Hu,C., Lee,D., Chibbar,R.N. and van Huystee,R.B. (1987) *Physiol. Plant*, **70**, 99–102.

Ikehata,K., Buchanan,I.D., Pickard,M.A. and Smith,D.W. (2005) *Biores. Technol.*, **96**, 1758–1770.

Lige,B., Ma,S. and van Huystee,R.B. (2001) *Arch. Biochem. Biophys.*, **386**, 17–24.

Martínez,Á.T., Ruiz-Duenas,F.J., Martínez,M.J., Río,J.C. and Gutiérrez,A. (2009) *Curr. Opin. Biotechnol.*, **20**, 348–357.

Martinez,M.J., Ruiz-Duenas,F.J., Guillen,F. and Martinez,A.T. (1996) *Eur. J. Biochem.*, **237**, 424–432.

McEldoon,J.P. and Dordick,J.S. (1996) *Biotechnol. Prog.*, **12**, 555–558.
Mester,T. and Field,J.A. (1998) *J. Biol. Chem.*, **273**, 15412–15417.
Micsonai,A., Wien,F., Kernya,L., Lee,Y.H., Goto,Y., Refregiers,M. and Kardos,J. (2015) *Proc. Natl. Acad. Sci. USA*, **112**, E3095–E3103.
Pérez-Boada,M., Ruiz-Dueñas,F.J., Pogni,R., Basosi,R., Choinowski,T., Martínez, M.J., Piontek,K. and Martínez,Á.T. (2005) *J. Mol. Biol.*, **345**, 385–402.
Petersen,J.F., Kadziola,A. and Larsen,S. (1994) *FEBS Lett*, **339**, 291–296.
Reading,N.S. and Aust,S.D. (2000) *Biotechnol. Progr.*, **16**, 326–333.
Ruiz-Dueñas,F.J. and Martínez,Á.T. (2009) *Microb. Biotechnol.*, **2**, 164–177.
Ruiz-Dueñas,F.J., Morales,M., García,E., Miki,Y., Martínez,M.J. and Martínez,Á.T. (2009) *J. Exp. Bot.*, **60**, 441–452.
Ruiz-Duenas,F.J., Morales,M., Mate,M.J., Romero,A., Marinez,M.J., Smith, A.T. and Martinez,A.T. (2008) *Biochemistry*, **47**, 1685–1695.
Ruiz-Duenas,F.J., Morales,M., Perez-Boada,M., Choinowski,T., Martinez,M. J., Piontek,K. and Martinez,A.T. (2007) *Biochemistry*, **46**, 66–77.
Sambrook,J., Fritsch,E.F. and Maniatis,T. (1989) *Molecular Cloning: A Laboratory Manual*. Cold Spring Harbor, New York.
Sáez-Jiménez,V., Acebes,S., Garcia-Ruiz,E., Romero,A., Guallar,V., Alcalde, M., Medrano,F.J., Martínez,A.T. and Ruiz-Dueñas,F.J. (2016) *Biochem. J.*, **473**, 1917–1928.
Sáez-Jiménez,V., Acebes,S., Guallar,V., Martinez,A.T. and Ruiz-Duenas,F.J. (2015a) *PLoS One*, **10**, e0124750.
Sáez-Jiménez,V., Fernández-Fueyo,E., Medrano,F.J., Romero,A., Martínez,A. T. and Ruiz-Dueñas,F.J. (2015b) *PLoS One*, **10**, e0140984.
Schuller,D.J., Ban,N., Huystee,R.B., McPherson,A. and Poulos,T.L. (1996) *Structure*, **4**, 311–321.
Shiro,Y., Kurono,M. and Morishima,I. (1986) *J. Biol. Chem.*, **261**, 9382–9390.
Sutherland,G.R. and Aust,S.D. (1996) *Arch. Biochem. Biophys.*, **332**, 128–134.
Valderrama,B., Ayala,M. and Vazquez-Duhalt,R. (2002) *Chem. Biol.*, **9**, 555–565.
Verdin,J., Pogni,R., Baeza,A., Baratto,M.C., Basosi,R. and Vazquez-Duhalt, R. (2006) *Biophys. Chem.*, **121**, 163–170.